# Ruthenium nanoparticles supported on nitrogen-doped carbon nanofibers for the catalytic wet air oxidation of phenol

Artemiy B. Ayusheev [a], Oxana P. Taran [a,*], Ivan A. Seryak [a], Olga Yu. Podyacheva [a], Claude Descorme [b], Mishele Besson [b], Lidiya S. Kibis [a], Andrey I. Boronin [a,c], Anatoly I. Romanenko [d], Zinfer R. Ismagilov [a], V. Parmon [a,c]

[a] Boreskov Institute of Catalysis, Siberian Branch of the Russian Academy of Sciences, 5 pr. Lavrentieva, 630090, Novosibirsk, Russia
[b] Institut de recherches sur la catalyse et l'environnement de Lyon (IRCELYON), UMR 5256 CNRS - Université de Lyon, 2 Avenue Albert Einstein, 69626, Villeurbanne, France
[c] Novosibirsk State University, 2 Pirogova st., 630090, Novosibirsk, Russia
[d] Nikolaev Institute of Inorganic Chemistry, Siberian Branch of the Russian Academy of Sciences, 3 pr. Lavrentieva, 630090, Novosibirsk, Russia

ABSTRACT

The effect of nitrogen content in N-doped carbon nanofibers (N-CNFs) on the catalytic activity of Ru/N-CNFs in the wet air oxidation of phenol has been studied. The N-CNFs, irrespective of nitrogen content and Sibunit, are shown to be low active. In the case of Ru-containing catalysts, nitrogen in N-CNFs was found to be responsible for both the increased activity and stability of the catalysts toward deactivation. The XPS showed the formation of carbon-oxygen structures with hydroxyl (carbonyl) end groups blocking ruthenium on the surface of the catalysts without nitrogen. For the catalysts with nitrogen, the ruthenium nanoparticles were not blocked in the course of the reaction and mainly the carboxyl (carbonate) surface groups were formed. The nature of this effect is discussed.

© 2013 Elsevier B.V. All rights reserved.

## 1. Introduction

Wet air oxidation (WAO) is an attractive method for the treatment of concentrated wastewater streams compared with biological treatment techniques, which are ineffective when toxic effluents such as phenols are present [1–3]. However, conventional WAO usually requires high pressures (5–200 bar) and temperatures (150–325 °C), which result in a high capital investment and high energy consumption for operation. Oxidation efficiency can be improved (and reaction temperature can be reduced) by using homogeneous or heterogeneous catalysts [4–7].

Homogeneous catalytic systems composed of transition metal ions, in spite of their efficiency in the oxidation of various organics, have well-known drawbacks, e.g., the production of metal-containing waste sludge which is difficult to dispose, and the catalyst deactivation by some metal complexing agent. The promising heterogeneous catalysts for catalytic wet air oxidation (CWAO) are noble metal catalysts (Ru, Pt, Pd) supported on carbon materials, which are very effective and resistant to active component leaching [7]. The literature data on the activity of noble metals in CWAO of different organic pollutants are contradictory:

some authors consider Pt as the most active metal, whereas in other works Ru shows the highest activity [6,7]. However, taking into account the lowest cost of ruthenium among the mentioned metals, Ru-containing catalysts appeared to be the most promising for treatment of wastewaters.

Recently, some interest has been displayed in using carbon nanomaterials doped with nitrogen as metal catalyst supports [8]. Nitrogen introduction into the carbon structure opens up a good possibility to regulate the surface and electronic properties of carbon nanotubes, carbon nanofibers (CNFs) or graphene [9–13]. By now, a sufficient experimental material has been accumulated, making it possible to conclude that the use of nitrogen-doped carbon nanomaterials as metal catalyst supports increases the catalytic activity in electrochemical oxidation of methanol or hydrogen in fuel cells [14–18], selective hydrogenation of cinnamaldehyde [19,20], ammonia decomposition [21], isotope exchange [22], and CO oxidation [23]. The increase in catalytic activity is associated with several basic factors: (1) introducing a heteroatom into carbon material makes it possible to control the size of the supported metal particles and to obtain a narrower particle size distribution; (2) using a support of higher conductivity leads to enhanced chemical reactivity for electron transfer processes in a catalytic system; (3) there occur changes in the acid-base properties of the support surface.

In the literature, there are virtually no data on the application of nitrogen-doped carbon nanomaterials as catalysts or catalyst supports in the CWAO processes. Only in a recent work [24], aminated active carbon (AC) was studied as a catalyst in the CWAO of coking wastewater at 140–160 °C and 0.2–1 MPa of oxygen partial pressure. The ACs aminated at 450–650 °C showed a little higher activity than the parent untreated AC. Based on a higher surface content of nitrogen and a lower surface area of the aminated ACs compared to the parent one, the increase in the catalytic activity was attributed to the nitrogen-containing functional groups. However, it is presently unclear how nitrogen in the carbon structure can affect the performances of the graphite-like carbon nanomaterials and noble metals supported on carbon nanomaterials in the CWAO.

In this regard, the present work is focused on the study of the effect of nitrogen in nitrogen-doped carbon nanofibers (N-CNFs) on the catalytic activity of pure CNFs and Ru/N-CNFs in the CWAO of phenol, which is a typical wastewater contaminant.

## 2. Experimental

### 2.1. Catalyst preparation

Two types of graphite-like carbon supports were used: N-CNFs and commercial mesoporous carbon Sibunit® [25].

N-CNFs differing in nitrogen content (0, 2, 6.8 wt.%) were synthesized by decomposing $C_2H_4$, 50%$C_2H_4$/50%$NH_3$ or 25%$C_2H_4$/75%$NH_3$ gas mixtures, respectively over a 65Ni-25Cu-10Al$_2$O$_3$ (wt.%) catalyst at 550 °C for 1 or 3 h. The methodology is described in detail in [11]. The synthesized supports were treated with concentrated hydrochloric acid to remove the exposed catalyst particles and after that washed by distilled water until the absence of chloride in rinsing water. For comparison, the graphite-like carbon material Sibunit® was used in this work [25]. Before using, it was washed several times in boiling water and oxidized by a wet gas mixture ($O_2$/N = 1/5) [26]. The characteristics of carbon supports are presented in Table 1.

The supported Ru catalysts (1 and 3 wt.%) were prepared by deposition of Ru from aqueous solutions of $Ru(NO)(NO_3)_3$ on N-CNFs and Sibunit® using the incipient wetness impregnation technique described in detail in [27,28]. After impregnation, the samples were dried and reduced in flowing $H_2$ at 300 °C for 2 h.

### 2.2. Physicochemical methods

The conductivity of N-CNFs and Sibunit® was measured via the standard four-contact method [12], the nitrogen content in the N-CNFs was determined by elemental analysis, and the electronic state of atoms was studied by XPS. The XPS spectra were recorded on a photoelectron spectrometer ES-300 (KRATOS Analytical). The spectra were recorded using nonmonochromatic AlKα radiation (photon energy 1486.6 eV). Gold Au 4f$_{7/2}$ and copper Cu 2p$_{3/2}$ lines (binding energies of 84.0 and 932.7 eV, respectively) were used as a calibration standard for the spectrometer. The qualitative control of the surface chemical composition was carried out via survey spectra in the range of 0–1100 eV, with an energy resolution corresponding to the maximum sensitivity (analyzer transmission energy 50 eV and energy step 1 eV).

To analyze the quantitative composition and chemical state of the elements, narrow regions were recorded with the analyzer transmission energy 25 eV and energy step 0.1 eV. The quantitative analysis of the composition was made by calculating the integrated intensities of the corresponding narrow lines in the XPS spectra taking into account atomic sensitivity factors (ASF) for each element [29].

The electron microscopy images were obtained using a JEM-2010 (JEOL) instrument with accelerating voltage 200 kV and resolution 1.4 Å. For TEM studies, the samples were supported on a holey carbon film placed on a copper grid. The size distribution of ruthenium particles and their average size were determined from statistical analysis of the TEM images using 300–500 particles. The average size was calculated by the formula

$$d_l = \sum \frac{d_i}{N},$$

where $d_i$ is the measured diameter of a metal particle, and $N$ is the total number of the particles.

The textural properties of carbon supports and catalysts were studied by low-temperature $N_2$ adsorption at −196 °C using an ASAP-2400 instrument (Micromeritics, USA). The specific surface area ($S_{BET}$) was calculated according to the BET model.

### 2.3. Catalytic activity measurements

The catalytic activity was investigated in a 150-mL autoclave made of Hastelloy C276 (Autoclave Engineers) at a constant temperature and with intensive stirring (at 1200 rpm). As shown in [30], the stirring at that speed makes it possible to conduct CWAO processes in the kinetic regime. 75 mL of an aqueous solution of phenol with a required concentration and a catalyst (125 mg) were placed into an autoclave reactor. The reactor was purged with argon five times by the alternate raising of the gas pressure up to 10 atm and depressurization. Then the temperature was raised to a desired value. After the temperature was forced into the regime (ca. 0.5 h), the first sample of the reaction solution was taken and analyzed in order to determine the amount of phenol adsorbed on the surface of the catalysts. The determined concentration of phenol, which was never less than 97% of desired initial concentration, was considered as initial for CWAO. After that the gas mixture ($O_2/N_2 = 1/5$) pressure was set at 50 bar and the reaction was started. In the course of the reaction, samples of the reaction solution (1 mL) were taken every 30 min to obtain information on the reaction kinetics. The samples were filtered through the syringe nozzle with a cellulose acetate membrane (a pore diameter of 0.2 μm), and phenol concentration was analyzed by the high pressure liquid chromatography (HPLC) method using a Shimadzu Prominence LC-20 system equipped with a SPD-M20A diode-array detector (detection wavelength λ = 210 nm) and a Phenomenex Synergi Hydro-RP column (250 mm × 3.0 mm) thermostated at 30 °C. The eluent (65 vol.% $H_2O$ + 35 vol.% acetonitrile) was supplied at the 0.7 mL min$^{-1}$ flow rate. The content of the total organic carbon (TOC) was determined after experiment in filtered aliquots of the reaction mixture with a Total Organic Carbon Analyzer (TOC-VCSH, Shimadzu, Japan). The solutions after reaction were analyzed for the presence of ruthenium by inductively coupled plasma optical emission spectroscopy (ICP-OES) on an Optima 4300DV instrument (PerkinElmer, USA).

The entire experiment was repeated three times to check the reproducibility of results.

The conversion of phenol ($X_{PhOH}$) and that of total organic carbon ($X_{TOC}$) were calculated by the following formulae:

$$X_{PhOH}(\%) = \frac{C_{PhOH}^0 - C_{PhOH}}{C_{PhOH}^0} \times 100,$$

$$X_{TOC}(\%) = \frac{C_{TOC}^0 - C_{TOC}}{C_{TOC}^0} \times 100,$$

where $C^0$ is the initial concentration of the substrate in the solution, and $C$ is its current concentration.

To compare the catalytic properties of the samples, the catalytic activity ($A$, mmol L$^{-1}$ min$^{-1}$ g$_{cat}$$^{-1}$) was calculated as the

**Table 1**
Characteristics of carbon supports and Ru-containing catalysts based on Sibunit and N-CNFs.

| Support | % Ru | $S_{BET}$, m$^2$ g$^{-1}$ | $D$ pore, Å | $V$ pore, cm$^3$ g$^{-1}$ | $\sigma_{300K}$[c], S cm$^{-1}$ | <d> of Ru, nm |
|---|---|---|---|---|---|---|
| Sibunit | 0 | 350 | 51 | 0.44 | 25 | – |
| | 1 | 346 | 64 | 0.55 | – | 1.4 |
| | 3 | 306 | 64 | 0.49 | – | 1.5 |
| N-CNFs-0%N-1[a] | 0 | 210 | 81 | 0.47 | 6.4 | – |
| | 1 | 211 | 84 | 0.44 | – | 1.5 |
| | 3 | 199 | 84 | 0.42 | – | 1.3 |
| N-CNFs-2%N-1[a] | 0 | 300 | 116 | 0.88 | 1.8 | – |
| | 1 | 284 | 117 | 0.83 | – | 1.4 |
| | 3 | 265 | 113 | 0.75 | – | 1.5 |
| N-CNFs-6.8%N-1[a] | 0 | 260 | 114 | 0.73 | 0.7 | – |
| | 1 | 254 | 115 | 0.72 | – | 1.5 |
| | 3 | 226 | 130 | 0.74 | – | 1.4 |
| N-CNFs-0%N-3[b] | 0 | 270 | 92 | 0.62 | 2.6 | – |
| | 3 | 242 | 92 | 0.56 | – | 1.5 |
| N-CNFs-2%N-3[b] | 0 | 250 | 85 | 0.53 | 4.0 | – |
| | 3 | 206 | 92 | 0.47 | – | 1.6 |

[a] Duration of N-CNFs synthesis process was equal to 1 h.
[b] Duration of N-CNFs synthesis process was equal to 3 h.
[c] Electrical conductivity at 300 K, S cm$^{-1}$.

reaction rate related to a gram of catalyst. The reaction rate ($W$, mmol L$^{-1}$ min$^{-1}$) was calculated from the kinetic curve of the substrate concentration dependence on the time at low conversion values.

## 3. Results

### 3.1. Characterization of carbon supports and supported Ru catalysts

In the course of the work, two series of N-CNF samples differing in the duration of carbon support synthesis were used: samples containing 0, 2 or 6.8% of nitrogen and grown during 1 h (N-CNFs-1), and those containing 0 or 2% of nitrogen and grown during 3 h (N-CNFs-3). Earlier [11], we showed that the $S_{BET}$ dependence of N-CNFs on growth time at 550 °C has a maximum between 1 and 3 h and goes down when growth time is increased. Meantime, the reaction time does not influence significantly the nitrogen content in N-CNFs. For comparison, in this work we used graphite-like mesoporous carbon Sibunit®, which proved to be a good support for CWAO catalysts [28,31].

The textural characteristics of carbon supports and ruthenium supported catalysts are summarized in Table 1. All of the investigated carbon supports are mesoporous with the total volume of pores from 0.44 to 0.88 cm$^3$ g$^{-1}$. Similarly to [11], for N-CNFs-1 series the nitrogen-containing materials are characterized by enhanced BET surface area and total pore volume compared with undoped carbon nanofibers. In turn, the BET surface area and total pore volume of the samples N-CNFs-3 are comparable, but the samples differ in nitrogen content (0 and 2 wt.%). The deposition of 1% Ru does not result in a significant change of the samples texture. In the case of the catalysts containing 3% Ru, we observed a noticeable decrease in the specific surface area and pore volume.

The TEM study of supported Ru catalysts has shown that all samples contain metallic round shape particles of ruthenium, and the average size of these particles is from 1.3 to 1.6 nm (Fig. 1, Table 1). Thus, these results are in full agreement with the literature data on the possibility of obtaining ruthenium in a fine-dispersed state on the surface of carbon supports by the indicated method [28]. Also, the TEM data demonstrate that introducing of nitrogen into the carbon structure does not influence the distribution of ruthenium particles on its surface.

The commercial Sibunit® shows the maximum electrical conductivity (25 S cm$^{-1}$) among the carbon supports studied (Table 1). The electrical conductivity of N-CNFs-1 (N = 0, 2, 6.8 wt.%) decreases as the nitrogen content increases. For N-CNFs-3 (N = 0, 2 wt.%), the conductivity is observed to increase when nitrogen is introduced.

### 3.2. The catalytic properties of carbon supports, supported Ru catalysts and stability of Ru/N-CNFs in CWAO of phenol

In a number of recent publications, it has been found that the commercial active carbons are highly active in wet air oxidation of phenol in the absence of supported active metals [32–38]. Therefore, at the beginning we tested N-CNFs and Sibunit in CWAO of phenol at a temperature of 160 °C and at a pressure of 50 bar.

In the blank experiment, in the absence of any catalyst but in the presence of O$_2$/N$_2$ gas mixture. The phenol concentration was continuously monitored during of the 6-h period. The conversion of phenol upon blank experiments never exceeded 5% compared to initial concentration. We also performed the adsorption experiments in the presence of N-CNFs or Sibunit but in the absence of oxygen. The maximum phenol concentration decrease (attributed to adsorption) was observed during the first 30 min of the 6 h process and achieved a value of ca. 3%. It means that the adsorption capacity of carbon supports is ca. 30 mg g(C)$^{-1}$, which is quite in line with literature data on similar materials. Therefore, in all CWAO experiments the phenol concentration in a reaction solution was measured before filling the autoclave with O$_2$/N$_2$ gas mixture, as it is written in Section 2.3; this concentration was taken as $C_0$.

The N-CNFs, irrespective of the nitrogen content, as well as Sibunit demonstrate a low catalytic activity (Fig. 2). Our present and previous works [26,28,39] differ from the works by other authors [32–38]: before using carbon materials, we carefully washed them with an acid to remove surface metal impurities and controlled the contents of metals (Ni, Cu, Fe) on the surface of catalysts by XPS, and in the solution after the reaction by ICP-OES. Note that the contents of transition metals (Ni for N-CNFs and Sibunit, Cu for N-CNFs, and Fe for Sibunit) in solutions after reactions did not exceed the contents of the same metals in blank experiments. (A quantity of nickel, namely, no more than 0.8 µg L$^{-1}$, is washed off the surface of the autoclave.) At the same time, in all the literature works carbons with an appreciable ash content (up to 12 wt.%) were used,
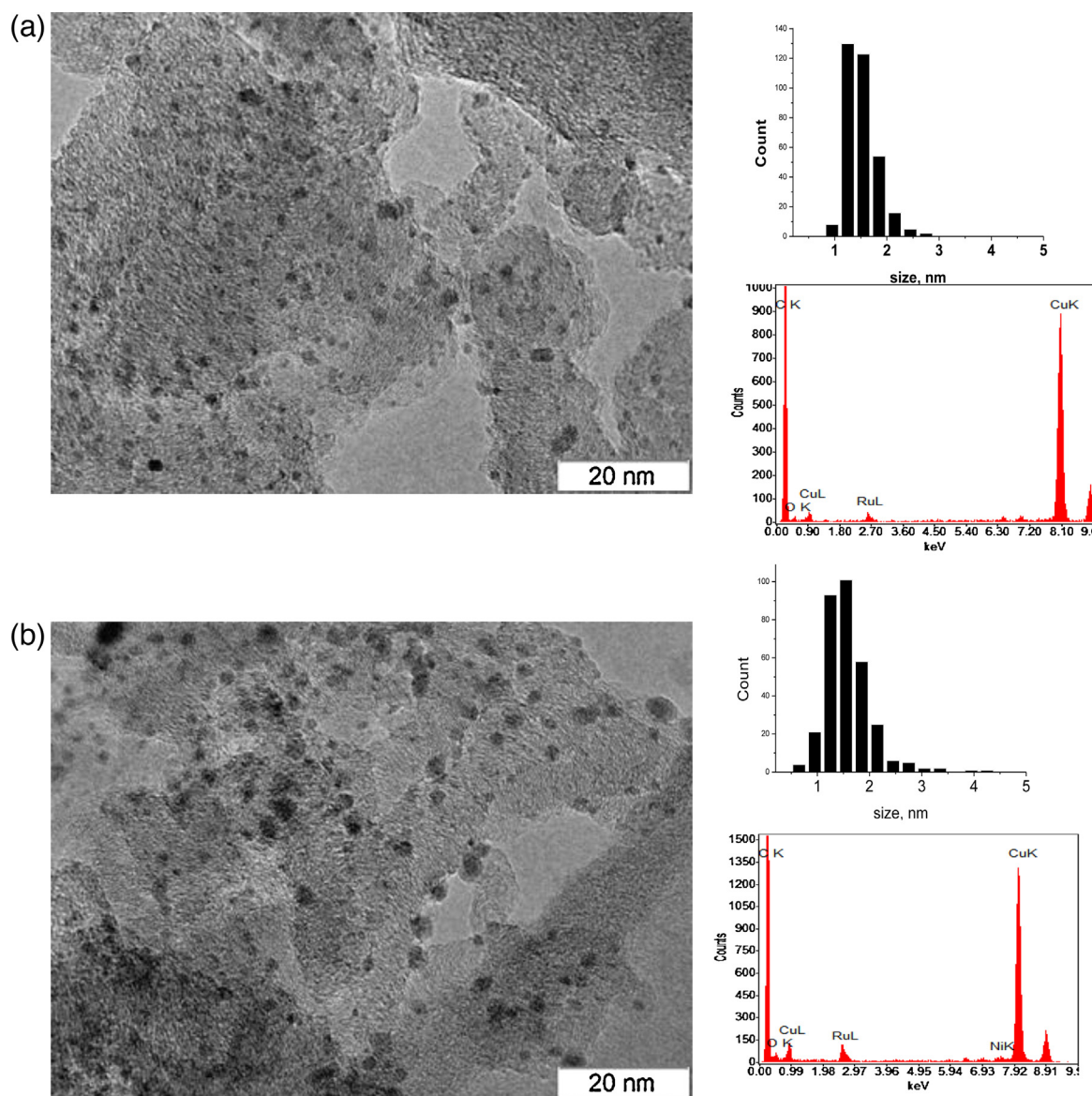
Fig. 1. TEM images, size distribution of Ru particles and EDX spectra of the catalyst: (a) 3% Ru/N-CNFs-0% N-3, (b) 3% Ru/N-CNFs-2% N-3.

and metal content in reaction solutions was not controlled. It seems that high concentration of metals in carbon support materials is responsible for their high catalytic activity.

The catalysts 1% Ru/N-CNFs-1 and 3% Ru/N-CNFs-1 were tested in CWAO of phenol at a temperature of 140 °C and at a pressure of 50 bar (Fig. 3). For comparison, under the same conditions we tested ruthenium catalysts supported on Sibunit (1% Ru/Sibunit and 3% Ru/Sibunit). Earlier, we have discovered a high catalytic activity of these catalysts in CWAO of phenol [28]. It is clear that deposition of ruthenium on carbon supports results in an increase of catalytic activity. The increase of nitrogen content in N-CNFs from 0 to 2 wt.% leads to a 1.5-fold enhancement of the supported catalyst activity (Fig. 3a). The increase of the nitrogen content to 6.8 wt.% is not accompanied by a further growth of the catalyst activity. The activity of the catalysts supported on Sibunit and the less active N-CNFs-0% N-1 was found to be close.

The differences in the observed activity of 1%- and 3%-Ru catalysts amounted to about 2.5 times. Taking into account the same dispersion of the Ru particles, one would expect a three-fold difference in the activities of 1% and 3% catalysts. Homogeneous oxidation of phenol and/or only low activity of the supports

themselves apparently made a small contribution to the observed activity. Note that TOC conversion over most of the studied catalysts is very close to phenol conversion (Fig. 3b and c). Only in the case of the most active catalysts (3% Ru/N-CNFs-2% N-1 and 3% Ru/N-CNFs-6.8% N-1), the selectivity to deep oxidation is lower (by 18 and 16%, respectively) than phenol conversion.

Ruthenium supported catalysts (3% Ru/N-CNFs-0% N-3 and 3%Ru/N-CNFs-2%N-3) were tested in 3 cycles of CWAO of phenol at 180 °C. The stability of catalysts is an important parameter for their practical application. The possible reasons for catalysts deactivation in CWAO process can be as follows: (1) leaching of an active component into the solution because the hot aqueous medium containing an oxidizer and organic acids, typical intermediates, is aggressive for most metals and oxides; (2) coking of the catalyst surface as result of the oxidative polymerization of phenol. For these reasons, more severe conditions, i.e. a higher temperature, were chosen for these experiments.

The results presented in Fig. 4 show that a catalyst supported on nitrogen-doped carbon nanofibers exhibits a higher activity than a catalyst supported on undoped carbon nanofibers in the three reaction cycles, and its catalytic properties remain unchanged from
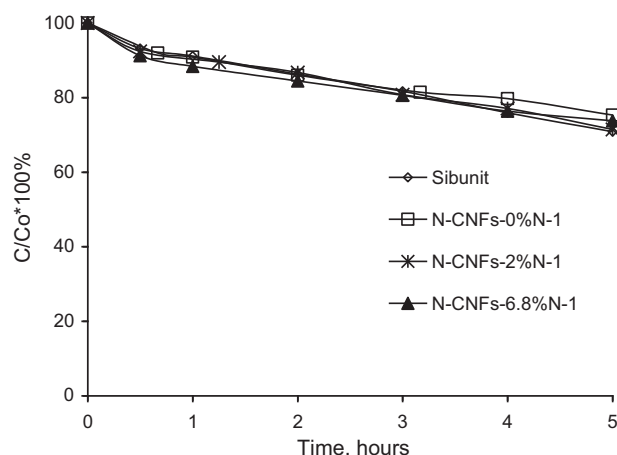
**Fig. 2.** Catalytic wet air oxidation of phenol by oxygen on Sibunit and N-CNFs-1 (0.02 M phenol, 1.67 g L$^{-1}$ catalyst, 160 °C, 50 bar total pressure).
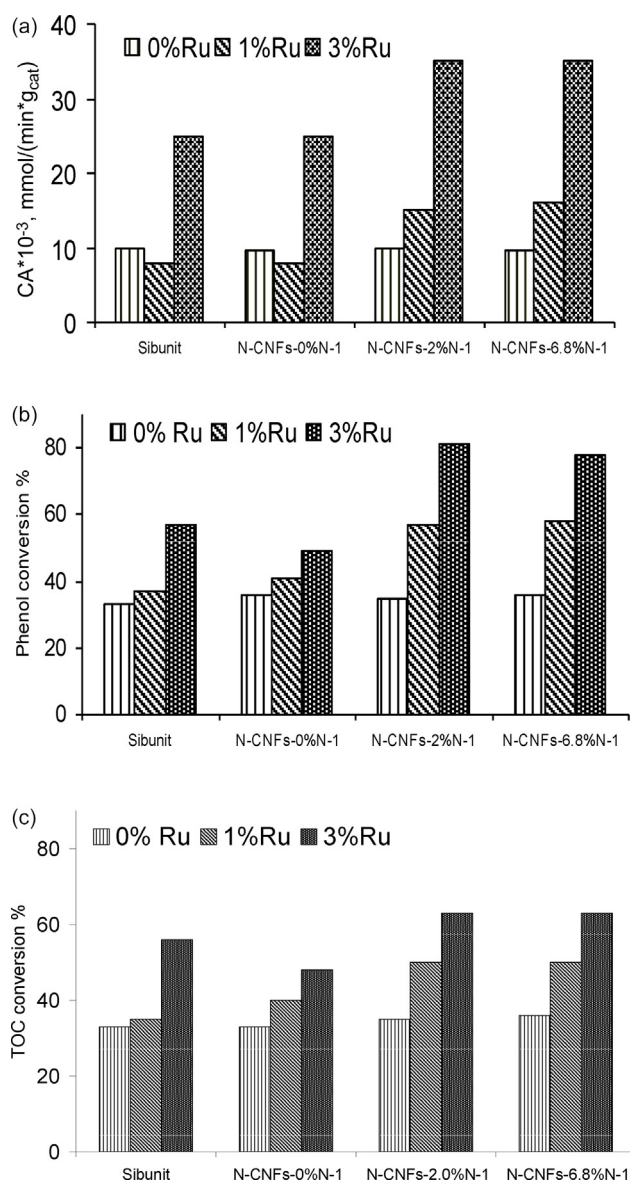


**Fig. 3.** Catalytic wet air oxidation of phenol on Sibunit, Ru/Sibunit, N-CNFs-1 and Ru/N-CNFs-1: (a) catalytic activity (CA), (b) phenol conversion after 6 h, (c) TOC conversion after 6 h (0.02 M phenol, 1.67 g L$^{-1}$ catalyst, 140 °C for Ru-containing catalysts and 160 °C for Sibunit and N-CNFs-1, 50 bar total pressure).

cycle to cycle. A catalyst on carbon nanofibers without nitrogen is already less active in the first cycle, and its activity in the 2nd and the 3rd cycles decreases. Besides, in the presence of the catalyst 3% Ru/N-CNFs-2% N-3 the 100% phenol conversion is observed, and TOC conversion after 6 h was high and almost constant: 92.3, 91.0, 93.0% for the 1st, 2nd and 3rd cycles. While in the presence of 3% Ru/N-CNFs-0% N-3 a complete phenol conversion was not achieved after 6 h, TOC conversion was lower and decreased from cycle to cycle: 89.1, 84.9 and 84.7% for the 1st, 2nd and 3rd cycles. The solutions after the reaction in last two cases have a light-yellow color. This proves the presence of products of the oxidative polymerization of phenol and its derivatives, which proceeds via the homolytic electron transfer mechanism with the production of phenoxy radicals [4].

Analysis of the solutions after the reaction did not show leaching of ruthenium.

### 3.3. XPS study of the catalysts

The XPS method was used for a quantitative and qualitative analysis of 3% Ru/N-CNFs-0% N-3 and 3% Ru/N-CNFs-2% N-3 catalysts, fresh ones and after the first cycle of the reaction.

The surface composition of the catalysts is given in Table 2. Note a considerable increase of oxygen content in the samples after the reaction due to formation of a large number of oxygen-containing groups. In the 3% Ru/N-CNFs-0% N-3 sample a decrease of the Ru/C ratio occurs (1.3% and 1.0% before and after the reaction, respectively). Since ruthenium is not leached into the solution and the size of its particles does not increase (according to the TEM data), it can be supposed that carbon–oxygen structures formed on the catalyst surface in the course of the reaction block the ruthenium nanoparticles. In the 3% Ru/N-CNFs-2% N-3 sample no change in the amount of ruthenium and nitrogen was observed on the catalyst surface after the reaction.

Fig. 5 shows the spectral region of carbon C 1s and ruthenium Ru 3d lines for initial supports and Ru catalysts before and after the reaction. Both for the supports and Ru-catalysts the carbon spectra are characterized by the main intensive peak in the region of 284.5–284.6 eV typical of the sp$^2$-hybrid carbon structures and a small satellite peak at ∼291 eV. The introduction of nitrogen into the carbon structure slightly increases the binding energy (BE) and broadens the peak, which correlates with our previous results [12,23]. After the reaction, the additional peaks appear in C1s spectra at ∼287 eV and ∼289 eV, which can be assigned to the formation of O-containing groups on the surface of carbon nanofibers, –OH and/or carbonyl ones (BE ∼287 eV) and carboxylic and/or carbonate ones (BE ∼289 eV) [29]. In the case of 3% Ru/N-CNFs-0% N-3 sample, the influence of the reaction mixture results in the formation of both hydroxyl (carbonyl) and carboxylic (carbonate) groups. And in the case of the 3% Ru/N-CNFs-2% N-3 sample, mainly the carboxylic (carbonate) groups are formed.

To analyze the state of ruthenium, the difference spectra technique was used. The C1s spectrum of the support was subtracted from the spectrum of a ruthenium-containing sample. In the difference spectra, the peak of Ru 3d$_{5/2}$ in the region of 281 eV is observed. This binding energy is higher than BE typical of metallic ruthenium (∼280 eV) and is close to the oxidized state of ruthenium in the composition of RuO$_2$ [40,41]. It must not be ruled out, however, that the shift of the ruthenium line toward higher binding energies compared to typical metallic Ru ones may be due to the so-called relaxation shift, which is observed in the case of the formation of very fine metal particles [42].

For a more detailed interpretation of the ruthenium electronic state, an analysis of the ruthenium line Ru 3p$_{3/2}$ was made (Fig. 6). For all the samples the main state of ruthenium is that with the binding energy ∼462.7 eV. This value of BE is intermediate

**Table 2**
Surface elemental composition of 3% Ru/N-CNFs-3 catalysts determined by XPS.

| Catalyst | C | | O | | N | | Ru | |
|---|---|---|---|---|---|---|---|---|
| | at.% | wt.% | at.% | wt.% | at.% | wt.% | at.% | wt.% |
| 3% Ru/0% N-CNFs-3 | 93.5 | 84.3 | 5.1 | 6.1 | n.a. | n.a. | 1.2 | 9.1 |
| 3% Ru/0% N-CNFs-3 after first cycle | 80.8 | 72.1 | 18.4 | 21.9 | n.a. | n.a. | 0.8 | 6.0 |
| 3% Ru/2% N-CNFs-3 | 91.6 | 81.4 | 4.8 | 5.7 | 1.8 | 1.9 | 1.3 | 9.4 |
| 3% Ru/2% N-CNFs-3 after first cycle | 81.9 | 71.7 | 15.0 | 17.4 | 1.6 | 1.6 | 1.2 | 8.5 |
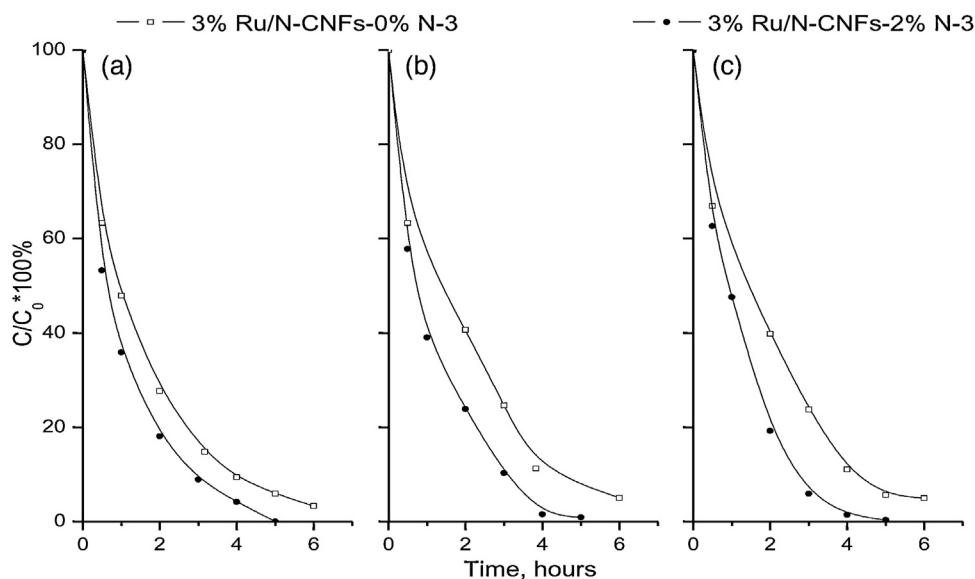


**Fig. 4.** Catalytic wet air oxidation of phenol over 3% Ru/N-CNFs-3 catalysts (a) first cycle; (b) second cycle; (c) third cycle (0.02 M phenol, 1.67 g L$^{-1}$ catalyst, 180 °C, 50 bar total pressure).

between the ruthenium state Ru$^0$ (461–462 eV [40,41,43]) and Ru$^{+4}$ (~463–464 eV [40,41,44]). Additional investigations of the samples containing bigger particles of ruthenium have shown that this shift toward higher binding energies relative to BE of metallic ruthenium is caused by a relaxation shift of the lines observed for fine particles of ruthenium. Also observed in the spectra of Ru 3p$_{3/2}$ is a peak of small intensity in the region of 466–467 eV, which according to the data from the literature can be attributed to the ruthenium hydroxides with a general formula RuO$_x$H$_y$ [43].

In the nitrogen spectra (see Fig. 7) one can see two main states with a binding energy ~398.5 eV and ~400.5 eV, which can be

assigned to pyridine nitrogen and graphite-like nitrogen, respectively [12,45,46].

The designation of peak with the binding energy of 398.5 eV to pyridine nitrogen is not in doubt. Concerning the attribution of N 1s peak with $E_b$(N 1s) = 400.5 eV, there is some discussion in the literature. In some papers the N 1s peak within the range 400.1–400.9 eV is assigned to pyrrolic-type nitrogen. It is necessary to note that the value of BE for nitrogen in similar group can vary up to 1 eV depending on the type of N-carbon materials, its structure, amount of defects and local environment of nitrogen atoms. So, the peak of pyrrolic-type nitrogen can overlap the peak of
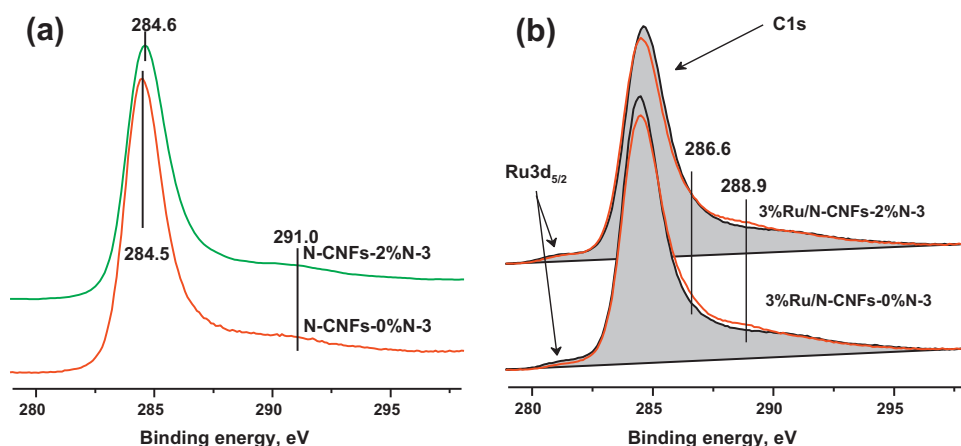


**Fig. 5.** C 1s spectra of (a) supports N-CNFs-3 and (b) 3% Ru/N-CNFs-3 catalysts (color-filled curves refer to initial catalysts, line curves – to catalysts after first reaction cycle). (For interpretation of the references to color in this figure legend, the reader is referred to the web version of this article.)
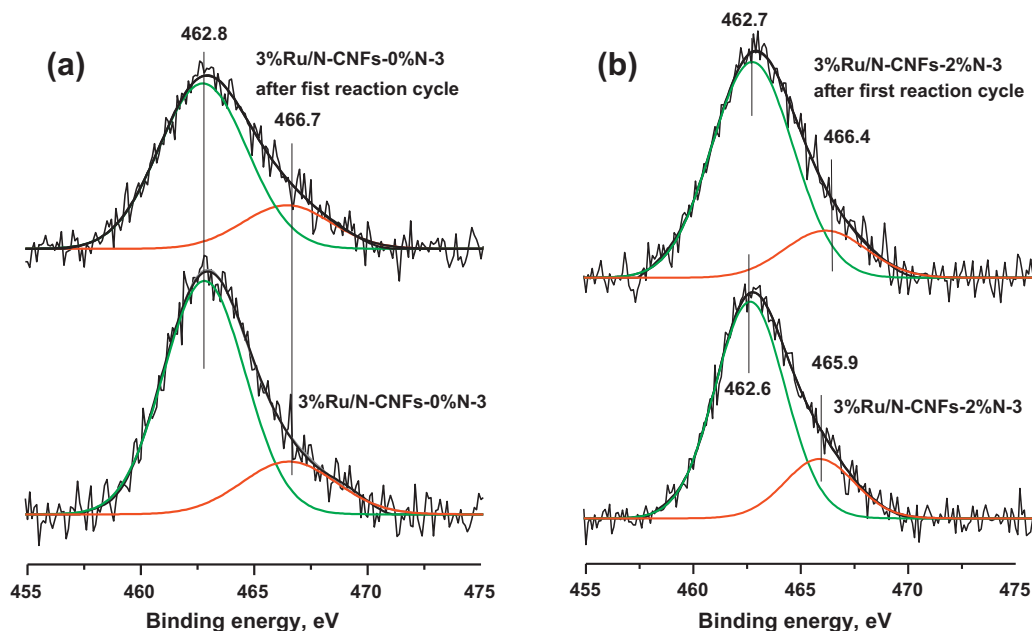
**Fig. 6.** Ru3p$_{3/2}$ spectra of (a) 3% Ru/N-CNFs-0% N-3, (b) 3% Ru/N-CNFs-2% N-3 for initial samples and samples after first reaction cycle.

graphite-like nitrogen. In the present work, no significant change in the N 1s spectra was observed between the fresh and cycled catalysts. Therefore no precise analysis of the nitrogen state was performed. However, according to our previous work, where the analysis of nitrogen states in the N-CNF materials was performed in detail [12], we assigned the peak around 400.5 eV to graphite-like nitrogen. Furthermore, as far as graphite-like nitrogen has a greater thermodynamic stability compared to pyrrolic-type N, it seems quite reasonable to assume that the most intensive peak in our N 1s spectra corresponds to graphite-like nitrogen.

In the O 1s spectra of the samples after the reaction, there occurs a considerable increase of intensity in the region of 531 eV characteristic of the hydroxyl and/or carbonyl groups and in the region of 532 eV typical of carbonate and carboxylic fragments [29].
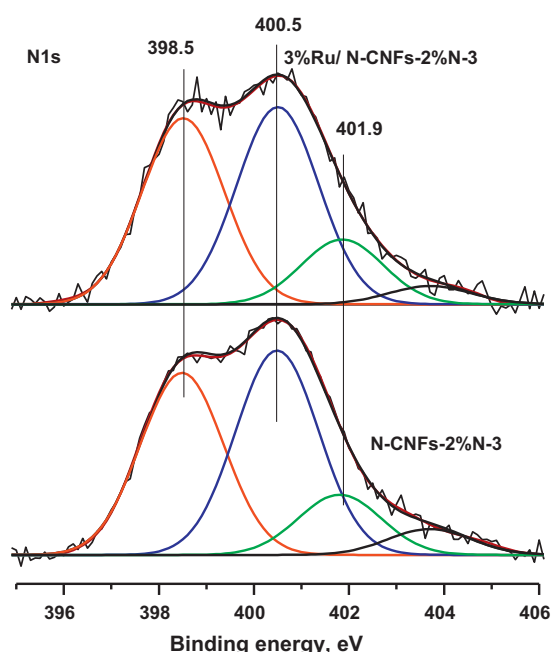


**Fig. 7.** N 1s spectra of N-CNFs-2% N-3 and 3% Ru/N-CNFs-2% N-3.

## 4. Discussion

In the present paper, the influence of a carbon support on the properties and catalytic activity of supported ruthenium catalysts in CWAO of phenol has been studied. Two different types of meso-porous carbon nanomaterials were used as supports: commercial Sibunit and N-CNFs. At present, the literature data on the influence of nitrogen in nitrogen-doped carbon nanomaterials on the catalytic properties of supported metallic catalysts are rather scarce and contradictory [14–23]. The available data suggest that the introduction of nitrogen into the carbon structure makes it possible (1) to control the size of deposited metallic particles, (2) to accelerate electron transfer in a catalytic system because of increased electrical conductivity of the support, and (3) to change the support surface properties. We have investigated the influence of all the three factors on the behavior of supported ruthenium catalysts in wet air oxidation of phenol at different temperatures (140 and 180 °C) and a pressure of 50 bar.

According to the results obtained, at 140 °C the catalytic activity changes in the following sequence: Ru/Sibunit ~Ru/N-CNFs-0% N-1 < Ru/N-CNFs-2% N-1 ~Ru/N-CNFs-6.8% N-1. The conversions after 6 h in the case of 1% Ru for 0% N-1 and 2% N-1 differ by 1.4 times, whereas in the case of 3% Ru by 1.6 times (Fig. 3b). These differences are more or less comparable. As the reaction temperature rises up to 180 °C, the activity of Ru/N-CNFs-2% N-3 exceeds that of Ru/N-CNFs-0% N-3 as well: in the 3rd cycle after 2 h the conversions differ by more than two times (Fig. 4). It was found for the 1–3% Ru/N-CNFs-1 series that the increase of nitrogen content in N-CNFs till 6.8 wt.% does not lead any further increase of the catalyst activity. However, for the 1–3% Ru/N-CNFs-1 series, nitrogen doping (2%) into the carbon structure is accompanied by a substantial increase of the BET surface area and pore volume, while the textural characteristics of the 1% Ru/N-CNFs-2% N-1 and 1% Ru/N-CNFs-6.8% N-1 are much closer (Table 1). So, it can be supposed that not only the nitrogen-doping of the support but also the textural properties of the catalyst influence the activity.

In our earlier work [23], with the 10% Pt/N-CNFs catalysts, it was demonstrated that as the nitrogen content in N-CNFs increases from 0 to 7.5%, the size of platinum particles decreases from 9 to 2 nm. In the present work, according to TEM data for the catalysts

1–3% Ru/N-CNFs, the introduction of nitrogen into the carbon structure does not influence the distribution of ruthenium particles on its surface, the average size of the particles varies from 1.3 to 1.6 nm, and the particles are in the metallic state. XPS also confirmed that Ru particles are in the metallic state. However, the observed binding energy of Ru $3p_{3/2}$ ~462.7 eV exceeds that of the standard metallic state of ruthenium by ~0.5 eV, which may be due to the relaxation line shift observed in the case of fine metallic particles [42]. Thus, one can assume that the decrease in the size of metallic particles with increasing the amount of nitrogen in the carbon support is observed only for highly concentrated supported catalysts [14,17,23]. However, in the case of catalysts with low contents of deposited metal this effect is not so evident [21].

The maximum conductivity among the studied carbon materials is demonstrated by the commercial Sibunit (25 S cm$^{-1}$, see Table 1), but at the same time the Ru catalyst on this support is the less active. The electric conductivity of N-CNFs-1 (N = 0, 2, 6.8 wt.%) synthesized for 1 h decreases as the nitrogen content increases, while the activity of deposited Ru catalysts increases if nitrogen-doped supports are used. For N-CNFs-0% N-3 and N-CNFs-2% N-3 synthesized for 3 h, there is a correlation between conductivity of the support and activity of the deposited catalyst. An analysis of the data available from the literature shows that the dependence of the electric conductivity on the content of nitrogen in nitrogen-doped carbon nanotubes [47] or N-CNFs [12] is non-monotonic. This type of dependence is determined by the fact that in the system there occurs a competition of the positive effect of doping an additional electron into the delocalized π-system of graphite-like material with the opposite effect caused by the order-disorder transformation of the carbon structure when a nitrogen atom is incorporated into this structure. However, in the present work, for N-CNFs-1 (N = 0, 2, 6.8 wt.%) synthesized for 1 h the electric conductivity decreases, while the specific surface area of the materials changes nonlinearly and amounts to 210, 300 and 260 m$^2$ g$^{-1}$. In [48], it was shown that with the standard 4-contact method, the electric conductivity increases with decreasing the specific surface area of the material. Besides, an increase in the compaction pressure of the same material from 0.5 to 10 MPa results in a three- to five-fold increase in the value of conductivity, which is connected with an increase in the number of contacts and a decrease in the free volume between particles. Hence, reliable values of electric conductivity can be obtained only for samples with the same texture and morphological properties. With this aim in view, in the present work we also studied catalysts using the supports N-CNFs-0% N-3 and N-CNFs-2% N-3 with close specific surface areas (270 and 250 m$^2$ g$^{-1}$), with the same morphology ("herringbone" structure), but with different amount of nitrogen (0 and 2 wt.%). As can be seen from Table 1, the introduction of nitrogen into CNFs is accompanied by an insignificant increase of conductivity from 2.6 to 4 S cm$^{-1}$. In this case, taking into account that the activity of 3% Ru/N-CNFs-2% N-3 exceeds that of 3% Ru/N-CNFs-0% N-3 and the activity of 3% Ru/Sibunit ($\sigma_{Sibunit}$ = 25 S cm$^{-1}$) is the least among the studied samples (Fig. 3), it can be concluded that the electrical conductivity do not influence directly the behavior of catalysts in the CWAO of phenol.

The most pronounced effect on the behavior of Ru/N-CNFs is exerted by a change in the surface state of the catalysts in the course of reaction. The results obtained in the present work allow a conclusion that the use of the N-CNF support enables one to increase not only the activity, but also stability of the ruthenium catalyst. Indeed, after the reaction, the surface concentration of Ru in the catalyst 3% Ru/N-CNFs-0% N-3 decreases by a factor of ~1.3, and for 3% Ru/N-CNFs-2% N-3 it remains constant. Besides, for 3% Ru/N-CNFs-0% N-3 the action of the reaction medium results in the formation of both hydroxyl (carbonyl) and carboxylic (carbonate) surface species. The presence of hydroxyl and carbonyl groups can testify that there

occur processes of additional hydroxylation of phenol with the formation of hydroquinone and pyrocatechol and their subsequent oxidation to form benzoquinones. Note that these substances are present on the chromatograms of the reaction mixture at the initial stages over low active catalysts. There may be further polymerization of phenols and intermediate phenol derivatives to form carbonaceous deposits of aromatic nature [6,49]. We cannot completely exclude the oxidation of the carbon support itself during the reaction. However, based on the literature [50] and our previous work [51], the oxidation of AC and graphite-like carbons under wet air, with the formation of significant amounts of oxygenates, proceeds at much higher temperature (>450 °C) compared to the operating temperature upon CWAO (140–180 °C). Furthermore, the formation of carbonaceous deposits of aromatic nature, containing hydroxyl and carbonyl groups, is also known from literature [6]. On the surface of 3% Ru/N-CNFs-2% N-3 the formation of mainly carboxylic (carbonate) groups is determined, which testifies to a deeper oxidation of phenol.

Taking into account that in the solution after the reaction no ruthenium is registered in all cases, i.e. it is not leached out, and the size of Ru particles does not increase, we can conclude that for 3% Ru/N-CNF-0% N-3 the decrease in intensity of Ru signal in XPS spectra and the formation of hydroxyl (carbonyl) groups are caused most likely by carbonization of the catalyst, which leads to ruthenium blocking and decreases its activity. The use of N-CNFs makes it possible to stabilize ruthenium particles in their initial state and thereby increase the catalytic activity. Explanation of the catalytic enhancement is a rather complicated task and requires further investigation. In the literature there is presently no commonly accepted point of view even on the mechanism of phenol WAO. Both free radical homolytic and heterolytic mechanisms were suggested [3]. The situation becomes more complicated when a catalyst is used, i.e. upon CWAO. Both Langmuir–Hinshelwood and Eley–Redeal models are proposed [4,6,7]. One of the most interesting models was suggested in [52]. This model, based on the Langmuir-Hinshelwood model, accounts for (i) the activation of pollutant through the formation of a surface complex and (ii) the dissociative oxygen adsorption on different types of active sites. In our case, the activation of oxygen can occur on the Ru nanoparticles, whereas the adsorption and the activation of phenol can proceed on the surface of the carbon support. In this case, the electron transfer from the substrate adsorbed on the carbon support to the Ru-oxygen active center (leading to abstraction of hydroxyl radical into solution) could be improved by N-doping of the carbon support. Therefore, one can suggest that the presence of nitrogen centers in N-CNFs accelerates local electron transfer in a catalytic system from the adsorbed molecules of the substrate to a catalytically active metallic center since only the carboxylic groups are formed on the surface and carbonyl groups are virtually absent. Thereby the reaction pathway could be changed from oxidative polymerization to the deep oxidation of phenol proceeding with rupture of the aromatic ring.

## 5. Conclusions

The influence of a carbon support (N-CNFs and commercial Sibunit) on the properties and catalytic activity of deposited ruthenium catalysts in the CWAO reaction has been investigated. The N-CNFs irrespective of nitrogen content and Sibunit are shown to be low active. The activity of Ru-containing catalysts at 140 °C varies in the following order: Ru/Sibunit ~Ru/N-CNFs-0% N < Ru/N-CNFs-2% N ~Ru/N-CNFs-6.8% N. At a reaction temperature of 180 °C the conversions on Ru/N-CNFs-2% N and Ru/CNFs-0% N differ by a factor of more than 2. The use of N-CNFs is found to exert no influence on the dispersion and electronic state of the deposited

ruthenium particles. It has been shown that the use of N-CNFs support makes it possible to increase the activity, and above all, the stability of the ruthenium catalyst to surface carbonization. The formation of carbon–oxygen structures with hydroxyl (carbonyl) end groups blocking ruthenium has been discovered for the catalysts without nitrogen. In the catalyst deposited on nitrogen-doped nanofibers, mainly the carboxylic (carbonate) groups are formed during CWAO. It is suggested that the presence of nitrogen centers in N-CNFs accelerates local electron transfer in a catalytic system, changing thereby the reaction pathway.

## Acknowledgements

## References

[1] V. Mishra, V. Mahajani, J. Joshi, Industrial and Engineering Chemistry Research 34 (1) (1995) 2.
[2] L. Liotta, M. Gruttadauria, G. Di Carlo, G. Perrini, V. Librando, Journal of Hazardous Materials 162 (2009) 588.
[3] S. Bhargava, J. Tardio, J. Prasad, K. Föger, D. Akolekar, S. Grocott, Industrial and Engineering Chemistry Research 45 (2006) 1221.
[4] J. Levec, A. Pintar, Catalysis Today 124 (2007) 172.
[5] F. Luck, Catalysis Today 53 (1999) 81.
[6] V.K. Kim, S. Ihm, Journal of Hazardous Materials 186 (2011) 16.
[7] F. Stüber, J. Font, A. Fortuny, C. Bengoa, A. Eftaxias, A. Fabregat, Topics in Catalysis 33 (2005) 3.
[8] L. Mabena, S. Ray, S. Mhlanga, N. Coville, Applied Nanoscience 1 (2011) 67.
[9] C. Ewels, M. Glerup, Journal of Nanoscience and Nanotechnology 5 (2005) 1345.
[10] M. Terrones, A. Jorio, M. Endo, A. Rao, Y. Kim, T. Hayashi, H. Terrones, J. Charlier, G. Dresselhaus, M. Dresselhaus, Materials Today 7 (2004) 30.
[11] A. Shalagina, Z. Ismagilov, O. Podyacheva, R. Kvon, V. Ushakov, Carbon 45 (2007) 1808.
[12] Z. Ismagilov, A. Shalagina, O. Podyacheva, A. Ischenko, L. Kibis, A. Boronin, Y. Chesalov, D. Kochubey, A. Romanenko, O. Anikeeva, T. Buryakov, E. Tkachev, Carbon 47 (2009) 1922.
[13] H. Wang, T. Maiyalagan, X. Wang, ACS Catalysis 2 (2012) 781.
[14] M. Saha, R. Li, X. Sun, S. Ye, Electrochemistry Communications 11 (2009) 438.
[15] H. Du, C. Wang, H. Hsu, S. Chang, U. Chen, S. Yen, L. Chen, H. Shih, K. Chen, Diamond and Related Materials 17 (2008) 535.
[16] T. Maiyalagan, B. Viswanathan, U.V. Varadaraju, Electrochemistry Communications 7 (2005) 905.
[17] T. Maiyalagan, Applied Catalysis B: Environmental 80 (2008) 286.
[18] R. Chetty, S. Kundu, W. Xia, M. Bron, W. Scuhmann, V. Chirila, W. Brandl, T. Reinecke, M. Muhler, Electrochimica Acta 54 (2009) 4208.
[19] J. Amadou, K. Chizari, M. Houlle, I. Janowska, O. Ersen, D. Begin, C. Pham-Huu, Catalysis Today 138 (2008) 62.
[20] X. Lepro, E. Terres, Y. Vega-Cantu, F.J. Rodriguez-Macias, H. Muramatsu, Y.A. Kim, T. Hayahsi, M. Endo, M. Torres, M. Terrones, Chemical Physics Letters 463 (2008) 124.
[21] F.R. Garcia-Garcia, J. Alvarez-Rodriguez, I. Rodriguez-Ramos, A. Guerrero-Ruiz, Carbon 48 (2010) 267.
[22] T. Kondo, T. Suzuki, J. Nakamura, The Journal of Physical Chemistry Letters 2 (2011) 577.
[23] O. Podyacheva, Z. Ismagilov, A. Boronin, L. Kibis, E. Slavinskaya, A. Noskov, N. Shikina, V. Ushakov, A. Ischenko, Catalysis Today 186 (2012) 42.
[24] H. Chen, G. Yang, Y. Feng, C. Shi, S. Xu, W. Cao, X. Zhang, Chemical Engineering Journal 198–199 (2012) 45.
[25] V. Likholobov, G. Centi, B. Wichterlová, A. Bell (Eds.), NATO Science Series. II. Mathematics, Physics and Chemistry, vol. 13, Kluwer Academic Publishers, Netherlands, 2001, p. 295.
[26] O. Taran, E. Polyanskaya, O. Ogorodnikova, V. Kuznetsov, V. Parmon, M. Besson, C. Descorme, Applied Catalysis A: General 387 (2010) 55.
[27] D. Pham Minh, G. Aubert, P. Gallezot, M. Besson, Applied Catalysis B: Environmental 73 (2007) 236.
[28] O. Taran, C. Descorme, E. Polyanskaya, A. Ayusheev, M. Besson, M. Besson, M. Besson, Catalysis in Industry 5, in press.
[29] J.F. Moulder, W.F. Stickle, P.E. Sobol, K. Bomben, Handbook of X-ray photoelectron spectroscopy, Perkin-Elmer Corporation, Physical Electronics Division, Eden Prairie Minnesota, 1992.
[30] P. Gallezot, S. Chaumet, A. Perrard, P. Isnard, Journal of Catalysis 168 (1997) 104.
[31] N. Dobrynkin, M. Batygina, A. Noskov, Catalysis Today 45 (1998) 257.
[32] A. Fortuny, J. Font, A. Fabregat, Applied Catalysis B: Environmental 19 (1998) 165.
[33] M. Suarez-Ojeda, F. Stuber, A. Fortuny, A. Fabregat, J. Carrera, J. Font, Applied Catalysis B: Environmental 58 (2005) 105.
[34] M. Santiago, F. Stüber, A. Fortuny, A. Fabregat, J. Font, Carbon 43 (2005) 2134.
[35] M. Suarez-Ojeda, A. Fabregat, F. Stüber, A. Fortuny, J. Carrera, J. Font, Chemical Engineering Journal 132 (2007) 105.
[36] A. Ayude, T. Rodriquez, J. Font, A. Fortuny, C. Bengoa, A. Fabregat, F. Stüber, Chemical Engineering Science 62 (2007) 7351.
[37] C. Ayral, C. Julcuor Lebique, F. Stüber, A. Wilhelm, H. Delmas, Industrial and Engineering Chemistry Research 49 (2010) 10707.
[38] N. Dobrynkin, M. Batygina, A. Noskov, P. Tsyrulnikov, Topics in Catalysis 33 (2005) 69.
[39] O. Taran, E. Polyanskaya, O. Ogorodnikova, C. Descorme, M. Besson, V. Parmon, Catalysis in Industry 3 (2011) 161.
[40] T. Hsieh, Ch. Chuang, W. Chen, J. Huang, W. Chen, Ch. Shu, Carbon 50 (2012) 1740.
[41] J. Gomez de la Fuente, F. Perez-Alonso, M. Martınez-Huerta, M. Pena, J. Fierro, S. Rojas, Catalysis Today 143 (2009) 69.
[42] G. Wertheim, S. DiCenzo, Physical Review B 37 (1988) 844.
[43] R. Chetty, W. Xia, Sh. Kundu, M. Bron, Th. Reinecke, W. Schuhmann, M. Muhler, Langmuir 25 (2009) 3853.
[44] B. Folkesson, Acta Chemica Scandinavica 27 (1973) 287.
[45] Zh.-H. Sheng, L. Shao, J.-J. Chen, W.-J. Bao, F.-B. Wang, X.-H. Xia, ACS Nano 5 (2011) 4350.
[46] Y. Xue, B. Wu, L. Jiang, Y. Guo, L. Huang, J. Chen, J. Tan, D. Geng, B. Luo, W. Hu, G. Yu, Y. Liu, JACS 134 (2012) 11060.
[47] J. Wiggins-Camacho, K. Stevenson, The Journal of Physical Chemistry C 113 (2009) 19082.
[48] D. Sebastian, I. Suelves, R. Moliner, M.J. Lazaro, Carbon 48 (2010) 4421.
[49] S. Keav, A. Martin, J. Barbier, D. Duprez, Comptes Rendus Chimie 13 (2010) 508.
[50] I.A. Kuzin, B.K. Strashko, Russian Journal of Applied Chemistry 39 (1966) 603 (in Russian).
[51] O.P. Taran, E.M. Polyanskaya, O.L. Ogorodnikova, C. Descorme, M. Besson, V. Parmon, Catalysis Industry 2 (2010) 381.
[52] A. Pintar, J. Levec, Chemical Engineering Science 9 (1994) 4391.